Howard Hughes Medical Institute

Published as: *Nat Methods*. 2015 March ; 12(3): 215–218.

Fixation-resistant photoactivatable fluorescent proteins for correlative light and electron microscopy

Maria G. Paez Segala[1], **Mei G. Sun**[1], **Gleb Shtengel**[1], **Sarada Viswanathan**[1], **Michelle A. Baird**[2,3], **John J. Macklin**[1], **Ronak Patel**[1], **John R. Allen**[2,3], **Elizabeth S. Howe**[2,3], **Grzegorz Piszczek**[4], **Harald F. Hess**[1], **Michael W. Davidson**[2,3], **Yalin Wang**[1], and **Loren L. Looger**[1]

[1]Howard Hughes Medical Institute, Janelia Farm Research Campus, Ashburn, Virginia, USA

[2]National High Magnetic Field Laboratory, Florida State University, Tallahassee, Florida, USA

[3]Department of Biological Science, Florida State University, Tallahassee, Florida, USA

[4]National Heart, Lung and Blood Institute, Bethesda, MD, USA

Abstract

Fluorescent proteins facilitate a variety of imaging paradigms in live and fixed samples. However, they cease to function following heavy fixation, hindering advanced applications such as correlative light and electron microscopy. Here we report engineered variants of the photoconvertible Eos fluorescent protein that function normally in heavily fixed (0.5–1% OsO_4), plastic resin-embedded samples, enabling correlative super-resolution fluorescence imaging and high-quality electron microscopy.

Fluorescent proteins (FPs) have revolutionized microscopy [1]. Some FPs are photoactivatable [2], meaning that they switch between dark and bright states or convert between two differently colored states. Photoactivatable FPs have enabled the "super-resolution" [3] imaging modality photoactivation-localization microscopy (PALM, also FPALM) [4, 5]. Serial photoconversion, imaging and bleaching of small sets of FP emitters allows accurate localization determination. Many PALM experiments employ the coral-

Correspondence should be addressed to L. L. L., loogerl@janelia.hhmi.org.

CONSTRUCT AVAILABILITY AND ACCESSION CODES

Plasmids encoding mEos4a and mEos4b as N- and C-terminal fusion proteins, as well as for bacterial expression, are available from Addgene (addgene.org; #51072-51073, #54810-54814). Other fusion proteins are available upon request. GenBank accession #s are: 1690171 (mEos4a) and 1690236 (mEos4b).

AUTHOR CONTRIBUTIONS

M.G.P.S. and L.L.L. conceived the project and designed mutations. M.G.P.S. made mutants, designed and implemented the *in vitro* screens, performed cell culture and light microscopy, and primary-fixed samples for EM. M.S. and Y.W. prepared samples for PALM/EM and performed TEM. G.S. and H.F.H. performed PALM imaging and quantification, SEM and CLEM data registration. S.V. assisted in mutation discovery. M.A.B., J.R.A., E.S.H. and M.W.D. constructed and screened fusion proteins. J.J.M. and R.P. performed photophysical characterization of variants. G.P. performed AUC characterization. M.G.P.S. and L.L.L. managed the project. M.G.P.S., MS and L.L.L. wrote the manuscript, with the help of the other authors.

SUPPLEMENTARY MATERIAL

Supplementary Material for this paper is available on the Nature Methods website.

COMPETING FINANCIAL INTERESTS

The authors have no competing financial interests.

derived green-to-red photoconvertible fluorescent protein EosFP [6] or its derivatives. After initial development of monomeric EosFP (mEos) [7], rational design produced mEos2 [8] and subsequently mEos3.1/3.2 [9], with iteratively improved folding, brightness, photostability and monomericity. These proteins facilitate imaging of live [10] and mildly fixed samples.

Correlative light and electron microscopy (CLEM) combines ultrastructural information from electron microscopy (EM) and localization data from fluorescence, which can be targeted to specific fusion proteins or organelles. However, all existing FPs are destroyed by exposure to osmium tetroxide (OsO_4) [4] at concentrations typically used to preserve cellular ultrastructure for EM (0.5–1%). In addition to decreasing FP fluorescence, OsO_4 particularly affects photoconversion, even at trace levels. Thus the use of FPs in CLEM has relied on weak chemical fixation (<0.001% OsO_4), which is not optimal for ultrastructure preservation [11]. Some methods preserve ultrastructure without OsO_4, but at the expense of resin compatibility, thus precluding serial-sectioning of large samples [12, 13]. For samples less than 500 nm thick, the combination of PALM imaging of photoactivatable GFP and cryo-electron tomography (CET) has recently been demonstrated in cryo-preserved cells (without any chemical fixation) [14]. Large samples such as brains, however, will require techniques compatible with resin embedding and sectioning.

Here we demonstrate two “mEos4” variants of EosFP with improved resistance of fluorescence and photoconversion to OsO_4 fixation. These new variants allow super-resolution PALM visualization of organelles and fused proteins in the context of well-preserved ultrastructure in both transmission EM (TEM) and scanning EM (SEM). Photophysical properties of the mEos4 probes in 0.5–1% OsO_4-fixed tissue are comparable to those of mEos2 in typical PALM preparations. Additionally, the probes show greater thermodynamic stability than mEos2, and one is more monomeric.

Previously, EosFP was demonstrated to function in PALM imaging in cryosections with subsequent TEM imaging [4]. EPON epoxy resin is a preferred embedding material for EM, given its superb ultrastructure preservation and excellent sectioning. However, EPON is incompatible with water, seemingly precluding FP fluorescence. Recently, the hydrophilic resin glycol methacrylate (GMA) was shown to preserve EosFP fluorescence, allowing correlative PALM and EM in resin-embedded samples, albeit requiring <0.001% OsO_4 [11]. We adopted this GMA embedding protocol with modifications (*e.g.* higher GMA concentration, less water), both for general use and for OsO_4 compatibility (**Methods**).

To optimize primary fixation conditions, Chinese hamster ovary (CHO) cells were transfected with constructs expressing mEos2-paxillin and subsequently treated with a number of fixatives, alone and in combination (**Methods**). Of the treatments tested, 4% paraformaldehyde (PFA)/0.2% glutaraldehyde best balanced mEos2 fluorescence preservation, paxillin distribution, low autofluorescence [15] and cellular structure preservation (Supplementary Fig. 1). TEM ultrastructure preservation of untransfected CHO cells fixed in these conditions and embedded in GMA or EPON was also compared (Supplementary Fig. 2). Mutants of mEos2 were produced and tested by incubation with increasing OsO_4 concentrations in a 96-well plate assay with purified protein (Fig. 1a,b, Supplementary Table 1). Variants designated mEos4a and mEos4b survived purified-protein

OsO_4 incubation much better than mEos2, mEos3.1 and mEos3.2 [9], both in the green (Fig. 1a) and photoconverted red (Fig. 1b) states. Subsequently, we transfected CHO cells with mitochondrially targeted mEos2, mEos4a or mEos4b. Transfected cells were post-fixed with 0 or 1% OsO_4 and embedded in GMA for light and electron microscopy (Fig. 1c,d). mEos2 fluorescence showed no survival with 1% OsO_4, whereas both mEos4 variants showed strong fluorescence localized to mitochondria (Fig. 1c), with good preservation of EM ultrastructure (Fig. 1d). OsO_4 resistance in the purified protein assay was lower than in a cellular context, likely because OsO_4 has many targets in the latter but only Eos in the former. In addition to improved OsO_4 resistance, the new variants exhibited better thermodynamic stability (Supplementary Fig. 3), monomericity (Supplementary Fig. 4) and performance in protein fusions (Supplementary Fig. 5) than mEos2. Purified-protein photophysics were identical to mEos2 (Supplementary Table 2). A sequence alignment of the variants and related FPs is shown in Supplementary Fig. 6.

We next tested mEos4 performance following expression in living cells. Both mEos4 variants showed good performance in tracking microscopy and were comparable to mEos2 in PALM, with similar numbers of total emitted photons (Supplementary Fig. 7). For CLEM, two techniques were used: a “consecutive-section” approach, in which adjacent sections were imaged by PALM and EM, respectively (Fig. 2); and a “same-section” approach, in which individual sections were imaged first by PALM and then by EM (Fig. 3). Both approaches allow for reasonable alignment of the PALM and EM frames by hand. The same-section approach, though, is further compatible with the use of gold nanoparticles, which are both fluorescent and EM-dense, as fiducial markers [16] (**Methods**). This allows precise registration with low and quantifiable error. mEos4b fused to the nuclear laminar protein lamin A (“lamin A-mEos4b”) was transfected into 3T3 cells and allowed to express, after which cells were primary-fixed as before, secondary-fixed with 1% OsO_4 and uranyl acetate (UA), dehydrated and embedded in GMA, sectioned and transferred to EM grids and glass coverslips (Fig. 2a). TEM produced high-contrast images, with well-preserved membranes, mitochondria (cristae clearly resolved) and other cellular structures. PALM yielded large fluorescence counts, with low background and clear labeling of the nuclear membrane (Fig. 2b). The two images were registered by hand, with fluorescence aligning to the nuclear envelope bilayer, as expected.

As an illustration of the same-section approach, we first repeated the experiment shown in Fig. 2 with primary fixation followed by high-pressure freezing/freeze substitution (HPF-FS) with 0.5% OsO_4, GMA embedding, PALM and subsequent post-staining and TEM (Fig. 3a). Quality of PALM and EM images from the same-section (Fig. 3b) and consecutive-section (Fig. 2b) approaches was similar. The important advantage of this method is that it enables precise image registration with low, quantifiable error (typically ~5 nm, see **Methods**), enabling quantitative correlative localization analysis of PALM and EM. Subsequently, we demonstrated generality of the same-section method by imaging mitochondrially-targeted mEos4a in PALM and both TEM and SEM (Fig. 3c). As before, ultrastructure preservation allowed clear resolution of membrane bilayers, mitochondrial cristae, chromatin and other organelles. Super-resolution localization of the mEos4a probe showed it in the intracristal matrix, as expected from fusion to a matrix-targeting tag.

Localization precision of mitochondrial mEos4a and lamin A-mEos4b (Fig. 3) in 0.5% OsO_4 were similar to mEos2 without OsO_4 (Supplementary Fig. 8). Given the success of the mEos4 variants in GMA, we subsequently tested them in EPON, but they did not survive (Supplementary Fig. 9). We also tested the resistance of the photoconverted red species to OsO_4; it did not survive 1% OsO_4 (Supplementary Fig. 10).

The fine localization of target proteins/organelles/cells is a common goal in biology. There are a number of techniques, each with its own strengths and weaknesses. Broadly speaking, structures can either be localized by endogenous expression of a contrast agent or by exogenous addition of contrast through antibodies and other affinity reagents. Cells of interest can also be directly injected with molecules such as Lucifer Yellow or biocytin, but this is only amenable to a few cells at a time.

The choice of labeling method will depend on constraints of the sample and goals of the experiment. Endogenous expression of contrast permits *in vivo* and time-lapse imaging, but requires tagging, which may disrupt function and/or localization, particularly under over-expression conditions. Fusing or targeting oxidases like horseradish peroxidase (HRP) [17] or APEX [18] allows the creation of EM-dense deposits following incubation with substrates like diaminobenzidine (DAB). However, substrate addition is difficult and uneven, typically leading to poor staining. Also, diffusion of the polymerized DAB limits utility of these enzymes for protein localization, but permits organelle or whole-cell filling and tracing. The designed oxidase miniSOG [19] is additionally fluorescent, facilitating CLEM, although not with optical super-resolution. Proteins can instead be tagged with epitopes and followed by immunohistochemistry.

Bringing in exogenous contrast from antibodies requires no tag fusion, but instead necessitates thin sectioning, permeabilization and long incubation times for penetration. Few antibodies work well in resin, and fewer work well on OsO_4-preserved tissue. Super-resolution imaging is achievable with antibodies to native proteins in several ways. Antibodies may be labeled with photoswitchable small molecule dyes, enabling STORM [20], or with gold nanoparticles for immuno-EM. Alternatively, ultra-thin sample sectioning by array tomography [21] enhances resolution.

Tagging proteins or organelles with FPs offers many options. Super-resolution microscopy is even possible *in vivo*, with techniques such as stimulated emission depletion [22], using reversibly photoswitchable proteins such as Dronpa [23] and IrisFP [24]. Cryo-preservation of samples without fixation largely retains structures in their native state, and enables correlative PALM and CET with photoactivatable GFP. Alternatively, samples may be cryo-sectioned and imaged at room temperature with Eos [13]. Cryo-preservation retains good ultrastructure, particularly in the absence of sectioning, but is inherently limited to small, thin samples. On the other hand, chemical fixation preserves large samples indefinitely, but can disrupt some native structures by protein cross-linking. If the contrast agent is amenable to plastic resin embedding, then this allows serial thin-sectioning and reconstruction of large volumes. Plasticization also increases electron dose tolerance, as well as compatibility of preserved samples with tomography and heavy metal staining [25]. It is this regime in which the mEos4 probes will prove most useful.

The mEos4 labels enable both wide-field and super-resolution light microscopy in samples specifically prepared to preserve EM ultrastructure. The probes are bright, permitting fine spatial localization (~13 nm) in tissue that has undergone fixation by PFA, glutaraldehyde, 0.5–1% OsO_4 and UA, as well as plastic resin embedding. Correlative imaging will enable the super-resolution localization of target proteins in the context of full EM (both TEM and SEM) preservation of membranes, vesicles and other sub-cellular organelles. The compatibility with 0.5–1% OsO_4-fixed plasticized sections offers a straightforward extension to large-volume, serial-section samples, under either diffraction-limited and super-resolution imaging. Of the techniques reviewed above, only those that work in plastic resin can be scaled up to the samples of greatest interest to neuroscience, *i.e.* whole brains or large portions thereof. Such use could assist large-scale connectomics projects, which suffer from the inability to track cellular identity solely in EM. Adding a fluorescent marker to a sparse set of neurons would make neurite tracing more resistant to experimental difficulties such as folds, slice loss and humans or algorithm error. Fluorescence preservation in large tissue blocks would also facilitate selection of small target regions for EM data collection. Developing Eos (or other FP) variants that survive EPON will decrease the sectioning loss rate and somewhat improve ultrastructure preservation over GMA; both factors will assist in tracing thin axons and dendrites over many hundreds or even thousands of serial sections. Such tracing assistance has been previously demonstrated with Lucifer Yellow, but this is difficult, low-throughput and not genetically targetable. HRP and other oxidases offer some hope, but require substrate addition and product diffusion, which degrades resolution.

Which of the two sample-preparation methods and two probes shown here should experimenters use? The consecutive-section technique is easier and minimizes sample handling, whereas the same-section technique allows more precise, quantitative registration of light and electron microscopic images. This is a key advantage for the accurate reconstruction of small structures, such as axons and dendrites, both within individual PALM/EM frames and through serial sections of large samples. mEos4b is an effectively pure monomer, and should be considered first when target proteins are recalcitrant to fusion. On the other hand, mEos4a may be more appropriate for “filling” applications, where whole cells or organelles are marked with fluorescence. We also note that in our hands, both 0.5% and 1% OsO_4 produced excellent cellular ultrastructure.

The mEos4 probes were engineered from mEos2 and mEos3.1/3.2 by rational design followed by medium-throughput *in vitro* screening. Their resistance to rigorous fixation validates the design goals of improved thermodynamic stability and reduced surface side-chain reactivity. In purified protein, the resistance of both the green and red states of mEos to OsO_4 were substantially increased by the mutations. For the green state, this resistance was sufficient to survive 1% OsO_4 fixation and resin embedding; for the red state, the degree of stabilization was insufficient. Further rounds of engineering may improve red-state resistance and/or EPON compatibility. Finally, it is likely that other FP scaffolds and enzymes (*e.g.* HRP) could be optimized by this protein-engineering paradigm.

ONLINE METHODS

Note: Additional Material is available on the Looger lab website: http://janelia.org/lab/looger-lab. Navigate to “Publications”, select this paper, and a link to the Additional Material will show up. References to this Additional Material are referred to below as “see website”.

Rational design of mEos4 variants—mEos2 was systematically mutated, primarily at surface positions, to simultaneously improve monomericity and fixation resistance by reducing surface reactivity and improving thermodynamic stability. First, a valine was added in the second position to improve Kozak translational efficiency [26]. Thermodynamic stability was greatly increased by addition of the mutations Phe34Tyr and Ser39Thr, and to a lesser extent by Ala69Val and Ile102Tyr (Supplementary Fig. 3). Both Phe34Tyr and Ser39Thr increase β-strand preference [27]; the Phe34Tyr mutation also increases hydrophilic character on the protein surface. Mutations to promote monomericity were designed to obstruct dimerization interfaces in the EosFP/mEos2 crystal structures [9,28] or taken directly from mEos3.1/3.2 [9]. The mEos3.2 mutations Ile102Asn/His158Glu/Tyr189Ala [9] improve monomeric performance (Supplementary Fig. 4). To a lesser extent, the Ile102Tyr mutation in mEos4a increases its monomericity relative to mEos2 (Supplementary Fig. 4). Monomericity of all mutants tested in this study is shown on the website. Fixation resistance was introduced by mutating reactive surface residues (Lys, His, Cys, Met) to preserve charge and size, while reducing nucleophilicity (typically Lys to Arg; His to Gln or Asn; Cys to Ala; Met to Leu). Lys9Arg and Cys195Ala each enhance fixation resistance, and the effects are additive (Fig. 1a, b and Supplementary Table 2). A single buried residue (Ala69) was mutated to Val improve chromophore packing; this mutation also appears in the Kikume fluorescent protein [29]. All tested mutants, initially with single amino acid substitutions and then with combinations, are shown in Supplementary Table 1. A sequence alignment of the engineered variants and related FPs is shown in Supplementary Fig. 6.

The mutations were combined into two “mEos4” variants: mEos4a=mEos2+Lys9Arg/Phe34Tyr/Ser39Thr/Ala69Val/Ile102Tyr/Cys195Ala and mEos4b=mEos2+Lys9Arg/Phe34Tyr/Ser39Thr/Ala69Val/Ile102Asn/His158Glu/Tyr189Ala/Cys195Ala. Both variants show high thermodynamic stability (Supplementary Fig. 3); improved monomericity relative to mEos2 (mEos4b being completely monomeric; Supplementary Fig. 4); bright and photostable green and red states, with good photoconversion between the two (Supplementary Table 2, see website); and resistance to fixatives (Fig. 1a,b and Supplementary Table 1). The probes were bright under both 1- and 2- photon excitation (see website). pH titrations of the mEos4 variants are similar to mEos2 (see website). Mutant Eos variants were produced in *Escherichia coli* with an affinity tag and purified according to standard protocols [8]. Protein characterization consisted of thermal denaturation (Supplementary Fig. 3); fluorescence polarization, gel filtration, and analytical ultracentrifugation measurements to determine monomeric character (Supplementary Fig. 4); cell-free assay of the incubation with OsO_4 in 96-well plates (Fig. 1a,b and Supplementary Table 1); and 1- and 2-photon spectroscopy (see website).

Purified protein testing—Mutants of mEos2 in the pRSETa vector (Invitrogen) were made by QuikChange (Agilent) or Kunkel [30] mutagenesis in *E. coli* XL1-Blue (Agilent). Point mutants were created first, with subsequent combination of beneficial mutations. Proteins were produced at 37 °C in *E. coli* BL21(DE3) grown in Studier auto-induction media [31] supplemented with 60 μg/ml ampicillin. Bacterial pellets were then re-suspended in 30 ml "native lysis" buffer (50 mM NaH_2PO_4, 300 mM NaCl, 10 mM imidazole, pH 8.0, adjusted with NaOH; protease inhibitors). Cell pellets were mechanically disrupted with an EmulsiFlex-C5 high-pressure homogenizer (Avestin). The supernatant was incubated overnight with 50% Ni-NTA resin (Bio-Rad) by rotating slowly on a rotary shaker, at 4 °C. The pre-equilibrated solution was carefully loaded onto an empty, clean 20 ml column (1.5 × 12 cm polypropylene; Bio-Rad), and purified by gravity-flow chromatography (batch purification). The flow-through was collected by washing 4 times with 20 ml "native wash" buffer (50 mM NaH_2PO_4, 300 mM NaCl, 20 mM imidazole, pH 8.0, adjusted with NaOH) and kept for SDS-PAGE analysis, followed by five to six 2 ml fractions collected in "elution" buffer (50 mM NaH_2PO_4, 300 mM NaCl, 250 mM imidazole, pH 8.0, adjusted with NaOH) and kept for SDS-PAGE analysis.

Spectroscopic characterization—Absorption spectra of purified proteins in 50 mM tricine, 100 mM NaCl buffer (pH 8.2) were measured with an absorbance spectrometer (Lambda 35, Perkin-Elmer). mEos2 was additionally measured in 50 mM MOPS, 100 mM NaCl (pH 7.2) for comparison to literature values. All protein solutions were first centrifuged (10,000 RPM for 5 minutes) to remove scattering particles, with the supernatant used for measurements. Protein concentration was determined by UV absorbance at 280 nm, using an extinction coefficient (in $M^{-1}cm^{-1}$)$\varepsilon_{280} = N_{Trp}*5500 + N_{Tyr}*1490 + N_{Cys}*125$. The extinction coefficient of the green form was determined by the measured absorbance at 505 nm divided by the protein concentration. The extinction coefficient of the red form was found by measuring the initial change in OD of the red and green forms of protein following irradiation with 385 nm light, assuming in an incremental time period the loss in concentration of green-form proteins by photoconversion equals the gain in concentration of red-form proteins. We accounted for the fact that the decrease in OD at 505 nm rides on top of the tail of the red-form absorbance. Fluorescence excitation and emission spectra were recorded on either a microplate reader (Safire^2, Tecan) or a luminescence spectrometer (LS55, Perkin-Elmer). Photoconversion on purified protein solutions was performed in cuvettes using a LED flood array (Loctite) operating at 385 nm (14 nm full-width at half-maximum) that delivered an intensity of 0.42 W/cm^2 at the sample face. Quantum yields were measured in an integrating-sphere spectrometer (Quantaurus, Hamamatsu) for both green-form and photoconverted red-form proteins (each solution 3 ml of 0.1 OD at peak absorbance).

Circular dichroism—CD experiments were performed on a Chirascan CD spectrometer (Applied Photophysics) with a 90w thermoelectric temperature controller (MTCA series) equipped with auto-tuning (Melcor). Far-UV spectra (190–240 nm) were obtained in quartz cuvettes of 1-cm path length (Hellma Analytics) with 0.3 ml of 3.5 μM Eos dialyzed into 10 mM sodium phosphate buffer, pH 7.4.

Time per point: 0.5 s. 38–39 temperature points were recorded from 20.0 to 95.0 °C in stepped ramp mode. Buffer-blank spectra, obtained under identical conditions, were subtracted. Signal at 200 nm (representing the β-barrel structure) is plotted.

Size-exclusion chromatography—Pure proteins were dialyzed into 25 mM tricine, 100 mM NaCl, pH 8.3. Gel filtration was performed using a Superdex 75 column (GE Healthcare) on the BioLogic LP purification system (Bio-Rad). Molecular weight standards (GE Healthcare) and sample solutions were mixed together in gel filtration buffer (150 mM Tris, 50 mM NaCl, pH 7.5), added to the column and eluted in 200 μl fractions collected into a well plate. 280 nm absorbance, 480/510 nm (5 nm /5 nm bandwidths) fluorescence, and 560/580 nm (5 nm/5 nm bandwidths) fluorescence were measured.

Fluorescence polarization assay—Pure proteins were dialyzed into 25 mM tricine, 100 mM NaCl, pH 8.3. All absorbance spectra, fluorescence spectra and fluorescence polarization data were obtained on a Safire^2 (Tecan) fluorimeter with UVStar 96 well plates (Greiner). Purified and buffer-exchanged samples were normalized by concentration with A_{280}. Concentrations ranging from 0–100 μM were analyzed, and absolute polarization was determined. Absolute polarization at 1 μM was taken as a proxy of oligomerization at endogenous expression levels.

Analytical ultracentrifugation—The centrifugation experiments were performed on a ProteomeLab XL-I analytical ultracentrifuge (Beckman Coulter) using interference optics. 0.4 ml samples were loaded into 12 mm path-length AUC cells, with dialysis buffer (50 mM tricine, 100 mM NaCl, pH 8.2) used as a reference. Samples were placed in the rotor and temperature was equilibrated in the centrifuge under vacuum for one hour after the set temperature of 20 °C had been reached. The rotor was accelerated to 50,000 rpm and scans were immediately started and recorded until no further boundary movement was observed. Data were analyzed in terms of continuous $c(M)$ distributions using the SEDFIT program [32].

Cell-free OsO_4 resistance assay—Pure proteins were dialyzed into 50 mM sodium phosphate buffer, pH 7.4, and normalized by concentration by A_{280}. A 4% (wt/vol) OsO_4 solution (Electron Microscopy Sciences) was diluted to a final concentration of 1%, and serial diluted in 96-well black fluorescence plates with clear bottom (Greiner). Pure protein was added to the serial dilution to a final concentration of 1 μM, and immediately sealed from the top with a clear seal (Bio-Rad). After incubation with OsO_4, fluorescence in both the green (Ex. 480 nm / Em. 515 nm; bandwidth 5 nm / 5 nm) and red (Ex. 550 nm / Em. 580 nm; bandwidth 5 nm / 5 nm) channels was measured from the bottom before and after conversion. Photoconversion was performed for half an hour on a Spectro-linker XL-1500 UV cross-linker, equipped with five 8-watt 365 nm tubes, each with a power of 5 mW/cm2 (Spectronics Corporation). Red signal after conversion was subtracted from red signal before conversion. Fluorescence was normalized to that in 0% OsO_4. For initial screening, only the green fluorescence channel was recorded, and OsO_4 concentration was held at 0%, 0.05% or 0.1%. The final variants and mEos2 were tested in a separate assay with more sample points, from 0 – 1% OsO_4.

Cell culture—All cell lines used in these experiments have been verified to be free from contaminating mycoplasma, viruses and other cells.

Performance in protein fusions—To assess the performance of mEos4a and mEos4b in live-cell imaging applications, a number of fusion proteins were constructed to the C- and N- termini of the mEos4 probes. All fusion proteins localized as expected, for example α-tubulin, CytERM and connexin-43 (Supplementary Fig. 5). Protein fusions were successful across all cellular compartments, including the cytoskeleton, nucleus, mitochondrion, endoplasmic reticulum, *etc*. (see website). Neither fluorescent protein affected the mitotic cycle when fused to histone 2B (Supplementary Fig. 7, see website). All Eos variants, fused to CytERM, were also tested in an "Organized Smooth Endoplasmic Reticulum" (OSER) assay, which is a sensitive method for detecting effective protein monomericity in fusions [33]. The new versions performed better than tdEos, mEos2 and dEos (Supplementary Fig. 5, see website). A number of fusion proteins were subsequently tested in PALM and photoconversion-tracking microscopy (Supplementary Fig. 7, see website).

Organized smooth endoplasmic reticulum (OSER) live-cell assay—To prepare the fusion vectors used for the live-cell OSER assay, the first 29 amino acids of rabbit cytochrome p450 (CytERM; XM_002718526.1) were ligated into a mEGFP-N1 (Clontech-style) cloning vector. The mEos4a and mEos4b fluorescent proteins were inserted downstream of the CytERM sequence using the AgeI and NotI restriction enzyme sites with a 17 amino acid linker (RILQSTVPRARDPPVAT). For this assay, HeLa (CCL-2, ATCC) cells were cultured as described below and seeded onto 35-mm culture dishes containing an 18 × 18 mm glass coverslip. The cells were maintained in a 5% CO_2 incubator for approximately 24 hours before they were transfected with 1 μg of the CytERM plasmid using Effectene (Qiagen). Transient transfections were visually assayed on an Olympus IX71 inverted microscope equipped with an Olympus LC Plan Fluor 40x dry objective (NA=0.60). To measure the monomeric character of the fluorescent protein fusions, the total number of cells in an individual field of view was counted, including the cells with morphologically normal ER as well as cells containing artifacts (stacked cisternae "whorls") [33]. Multiple fields of view were counted from several transfected dishes until a total of 10,000 cells had been counted. The percentage of "morphologically normal" cells was determined by dividing the smooth ER morphology by the total number of cells for each fluorescent protein fusion.

Construction of mammalian expression plasmids and cell culture—The mEos4 (mEos4a, mEos4b) fusion proteins were constructed using C1 and N1 (Clontech-style) cloning vectors. Utilizing PCR the mEos4a and mEos4b cDNAs were amplified with a 5′ primer encoding an AgeI site and a 3′ primer containing either a BspEI (C1) or NotI (N1) site for creating the C-terminal and N-terminal (with respect to the FP) cloning vectors. The PCR products were gel purified, digested, and ligated to identically treated EGFP-C1 and EGFP-N1 cloning vectors.

To construct the mEos4a/b fusions to the C-terminus of the fluorescent protein (number of linker amino acids in parenthesis), the subsequent digests were performed: human lamin A (18), NheI and BglII (cDNA source: D. Gilbert, FSU; NM_170707.2); human α-tubulin

(18), NheI and BglII (cDNA source: Clontech; NM_006082); human H2B (6), BglII and NheI (histones, cDNA source: G. Patterson, NIH; NM_021058.3). To prepare the N-terminal fusions to mEos4a, the following digests were performed: rat connexin-43 (7), BamHI and NotI (cDNA source: M. Falk, Lehigh U; NM_001004099.1); cytERM (17), AgeI and NotI (rabbit cytochrome p450, E. Snapp, Albert Einstein College of Medicine; XM_002718526.1). For the mitochondrial-targeted proteins, the N-terminal sequence ATGTCCGTCCTGACGCCGCTGCTGCTGCGGGGCTTGACAGGCTCGGCCCGGCGG CTCCCAGTGCCG CGCGCCAAGATCCATTCGTTG (MSVLTPLLLRGLTGSARRLPVPRAKIHSL), from human cytochrome c oxidase subunit 8A, followed by a linker GGGGATCCACCGGTCGCCACC (GDPPVAT) was cloned before mEos, using 5′ BamHI/3′ NotI. Following digestion with the appropriate restriction enzymes and gel purification, the plasmids were ligated together with the similarly digested and gel-purified mEos4a or mEos4b cloning vector and purified using a Plasmid Maxiprep kit (Qiagen).

For cell culture for EM experiments, we largely followed the protocol of Brown *et al.* [34]. Briefly, 35 mm glass bottom dishes (MatTek corporation) plates were pre-coated with 5–10 μg/ml fibronectin (Millipore) in 1x PBS (Gibco) before cells were plated. Chinese hamster ovary cells (CHO-K1, ATCC), adherent fibroblastoid cells (ATCCR CCl-61, cryopreserved) or 3T3 mouse fibroblast cells (Life Technologies) were used (specified in each experiment). CHO cells were maintained in complete basal growth medium: Dulbecco's Modified Eagle's Medium (DMEM)/F12 (Gibco) + 10% FBS (Gibco). 3T3 cells were maintained in DMEM, 10% (wt/vol) normal calf serum, 1 mM sodium pyruvate, 4 mM L-glutamine, 4.5 g/ml glucose, and 1.5 g/ml sodium bicarbonate. ~4×10^5 live CHO cells, and ~8×10^5 live 3T3 cells, were used per imaging well. For analysis of fixation conditions, untransfected cells were examined to measure background fluorescence. Transfected cells were measured to ensure retention of mEos fluorescence. Cells were transfected with 1 μg DNA per well using an Amaxa SF Cell Line 96-well electroporator with the Nucleofector kit (Lonza). After transfection, cells were moved to a 37 °C incubator. Cells were imaged 24 hours after transfection.

Primary fixation for light and electron microscopy—We first established a cellular assay in which fixative conditions could be tested for structure preservation, effect on EosFP fluorescence, and production of interfering background fluorescence. Chinese hamster ovary (CHO) cells were transfected with constructs expressing mEos2-paxillin and subsequently treated with a number of primary fixatives, alone and in combination (Supplementary Fig. 1). Cells were imaged and quantified for brightness of mEos2 in both the green and red channels. Cells with no FP were treated identically to assess background fluorescence. In parallel, fixatives were evaluated for overall cellular structure preservation. Cell culture medium was DMEM, with 4.5 g/l glucose and 110 mg/l sodium pyruvate added, with no Phenol Red added. For 3T3 cells (but not for others), 200 mM glutamine was also added. Most fixative treatments were discarded for high background fluorescence in green (*e.g.* Hand and Hassel), red (*e.g.* DTSSP) or both (*e.g.* 2.5% glut, ETA) channels; destruction of green Eos fluorescence (*e.g.* 2.5% glut); mislocalized Eos (*e.g.* DMS, DTSSP), or unacceptable cellular structure preservation (*e.g.* Zn, BS3). Of the treatments tested, 4%

PFA/0.2% glutaraldehyde best balanced Eos fluorescence preservation, low autofluorescence and structure preservation (Supplementary Fig. 1). Under these primary fixation conditions, mEos2 fluorescence decreased by ~30% in the green channel and ~40% in the red, with good distribution pattern, judged from fluorescence images. (See next section for detailed description of fixatives tested and image analysis methods.) Subsequently, untransfected cells (*i.e.* no mEos) were prepared according to several EM protocols [35] and checked for fine ultrastructure preservation (Supplementary Fig. 2). Conventional EM preparation (2% PFA, 2.5% glut, 1% OsO_4, EPON 12^{TM} resin) provided excellent ultrastructure (Supplementary Fig. 2c). We carried out systematic testing of EM conditions and were able to achieve good structural preservation with both conventional EM chemical fixation ("CCF"; Supplementary Fig. 2a-c) and high-pressure freezing/freeze substitution ("HPF-FS"; Supplementary. Fig. 2k-n). Increasing OsO_4 concentration improved structure (Supplementary Fig. 2f-j, k-m). At 1% OsO_4, ultrastructure in glycol methacrylate (GMA) resin (Supplementary Fig. 2k,m) was excellent equivalent to that in EPON resin (Supplementary Fig. 2b,n). In low OsO_4, neither resin showed particularly good ultrastructure. The use of free-aldehyde quenchers such as borohydride ($NaBH_4$) and cyanoborohydride ($NaCNBH_3$) [36] after chemical fixation (but before resin infiltration, *i.e.* pre-embedding) resulted in cellular damage, primarily through bubble formation (Supplementary Fig. 2d-e). However, when used in an optimized post-embedding procedure on resin section, they improved fluorescence imaging without adversely affecting structure (Figs. 2 and 3).

Analysis of fixatives and quenchers in light microscopy—For evaluation of fixatives in light microscopy, CHO cells were measured both untransfected and transfected with mEos2-paxillin. Cells were treated with the chemical mixture and then washed twice with 1x PBS before imaging. Images were taken on an Olympus IX81 motorized inverted fluorescence and differential interference contrast (DIC) microscope with a Hamamatsu Photonics C9100-02 EMCCD camera. Fluorescence filter cubes were a GFP cube for the green channel (473/31 nm//520/35 nm), and a Texas Red (562/40 nm//624/40 nm) cube for the red channel (Semrock).

For evaluation of preservation of overall cellular structure and paxillin localization, we used a U-Plan Fluorite 40x/1.3NA objective (Olympus). The CCD camera was saturated (16,384 in 14-bit mode) for the brightest image. Amplification gain was raised to 90–100 to decrease the exposure time to ~50 ms. Images were collected in both green and red channels.

For quantitation of background and mEos2 fluorescence, we used a U-Plan Fluorite 10x/0.3NA objective (Olympus). Images were collected as before, saved in 16-bit TIFF format and analyzed in IPlab (Scanalytics). For each image, 10 regions of interest (ROIs) were specified around cell bodies and 10 ROIs around empty portions of the dish. The average value of empty-dish fluorescence was used as a measure of autofluorescence of the fixative mixture itself, the dish and cellular debris. Each image was background-subtracted by this value. Background-subtracted fluorescence of untransfected cell bodies was taken as a measure of cell-bound autofluorescent species generated by the fixation reaction.

Fixatives and quenchers used in this study

Zinc fixative (BD-Pharmigen) [37]: 100 mM Tris buffer, 3 mM calcium acetate, 27 mM zinc acetate, 36 mM zinc chloride, pH 7.0.

Loman's fixative: 3.3′-dithiobis[sulfosuccinimidylpropionate] (**DTSSP**) (Thermo-scientific) [38]

Cells were washed 3 times with PBS buffer (100 mM sodium phosphate, 150 mM NaCl, pH 7.2). Subsequently, DTSSP was added to a final concentration of 1 mM, followed by 30 minutes incubation (or 2 hours on ice). Finally cells were washed 3 times with PBS, and at this point the aldehyde was added if also used, otherwise the stop solution (20 mM Tris, pH 7.5) was added for 15 minutes.

Bis[sulfosuccinidyl]suberate (BS3)(Thermo-scientific) [39]: Cells were washed 3 times with PBS buffer (20 mM sodium phosphate, 150 mM NaCl, pH 8.0). Subsequently, BS3 was added to a final concentration of 1 mM, followed by 30 minutes incubation (or 2 hours on ice). Finally cells were washed 3 times with PBS, and at this point the aldehyde mix was added if also used, otherwise the stop solution (20 mM Tris, pH 7.5) was added for 15 minutes.

Dimethylsuberidimate (DMS) (Thermo-scientific) [40]: Cells were washed 3 times with PBS, followed by the addition of 50 mM DMS diluted in 100 mM sodium borate buffer, 1 mM $MgCl_2$, pH 9.5. Finally cells were washed 3 times with PBS, and at this point the aldehyde mix was added if also used, otherwise the stop solution (100 mM glycine, pH 7.5) was added for 1 hour at room temperature.

Hassell and Hand method [41]: Cells were washed 3 times with PBS, followed by the addition of 50 mM DMS diluted in 100 mM Tris buffer, 200 mM $CaCl_2$, pH 9.5. Finally cells were washed 3 times with PBS, and at this point the aldehyde mix was added if also used, otherwise the stop solution (100 mM glycine, pH 7.5) was added for 1 hour at room temperature.

Quenchers: all of the quenchers were added to the cells after 3 washes of the aldehyde mix.

Ethanolamine (Sigma-Aldrich) [42]: 2 mM ethanolamine, pH 8.5 in water.

Glycine (Sigma-Aldrich)[42]: 100 mM glycine, pH 7.4 in PBS.

Tetrahydroborates (Sigma-Aldrich) [36,43]: Both $NaBH_4$ and $NaCNBH_3$ were used at a final concentration of 25–50 mM in PBS, pH 7.4. Samples were incubated on ice for 5 min, followed by replacement with fresh solution for another 5 minutes.

Sodium metaperiodate (Thermo scientific)[42,44]: (10 mM, in water) incubated for 30 min.

Epifluorescence microscopy—Filters used for fluorescence screening and imaging were purchased from Chroma Technology, Omega Filters or Semrock. To ensure proper

localization, mEos4a and mEos4b fusion proteins were characterized by transfection into HeLa (CCL2 line) and rat-kangaroo (PtK2) using Effectene (Qiagen) and ~ 1 μg vector. Transfected cells were grown on coverslips in a 1:1 mixture of DMEM and Ham's F12 supplemented with 12.5% Cosmic calf serum (Thermo Scientific). To verify localization and expression of the plasmids, the fusions were fixed after 48 hours in 2% (w/v) PFA (Electron Microscopy Sciences; Hatfield, PA), and washed twice in PBS containing 50 mM glycine before mounting with a polyvinyl alcohol/water-based medium. Epifluorescence images were captured with a Nikon 80i upright microscope coupled to a Hamamatsu Orca ER camera and a Semrock filter set to confirm proper localization.

Time-lapse imaging—The utility of photoconversion for time-lapse imaging and tracking of distinct protein populations was tested for several mEos4b fusions in transiently transfected epithelial cells (HeLa CCL2). Both the green and red species were sufficiently bright and photostable to allow for long-term time-lapse imaging. Photoconversion of mEos4b fused to H2B was used to dynamically track cell division. The exchange of photoconverted and native mEos4b labeling lamin A in the nuclear lamina was visualized over the course of several hours. Similar experiments were performed imaging actin dynamics and gap junction plaque growth behavior. All results are shown on the website.

Confocal microscopy—Laser-scanning confocal microscopy was conducted using an Olympus FV1000, equipped with argon-ion (457 and 488 nm) and helium–neon (543 nm) lasers and proprietary filter sets. Confocal imaging was performed in Delta-T culture chambers (Bioptechs) under a humidified atmosphere of 5% CO_2 in air.

PALM imaging of mEos4 variants fused to alpha-tubulin

Sample Preparation for PALM imaging—For PALM imaging, cells were seeded directly onto 35 mm, #0 thickness coverglass MatTek dishes (MatTek Corporation) approximately 24 hours prior to transfection. The culture medium was a 1:1 mixture of DMEM and Ham's F12 supplemented with 12.5% cosmic calf serum, as described above. Transfection was performed using the Effectene transfection reagent (Qiagen) following the manufacturer's instructions. Transfected cells were allowed to sit for approximately 24–48 hours prior to fixation, to ensure proper localization of the fusion construct. For α-tubulin fusions, cells were fixed in a 3% (w/v) PFA, 0.05% (v/v) glut, 0.3% (v/v) Triton X-100 solution in HEPES buffer, washed for approximately 5 minutes in a 0.1% solution of $NaBH_4$ in PBS on ice, and rinsed several times in PBS.

PALM Imaging—The potential of mEos4a, mEos4b and mEos2 for PALM was compared by imaging fusions of each FP to *alpha*-tubulin (Supplementary Fig. 7, see website). Hardware settings, including frame rate, gain, binning, *etc*., were identical for all acquisitions to facilitate comparison of images. Overall all three mEos variants performed similarly well in PALM imaging experiments, with large photon counts per molecule and many labeled molecules identified per run (Supplementary Fig. 7, see website).

PALM imaging of mEos4a, mEos4b and mEos2 fusion constructs was performed on a commercial Nikon (Nikon Instruments) N-STORM super-resolution system, featuring a

Nikon Eclipse Ti inverted research microscope with a motorized total internal reflection fluorescence (TIRF) illuminator. The instrument was operated in an oblique pseudo-TIRF mode, where signal is maximized by utilizing both TIR and reflected fluorescence. All imaging was performed using a Nikon 100X 1.49 NA Apo TIRF oil immersion objective and collected over a 40.96 μm × 40.96 μm area onto an Andor iXon 897 EMCCD camera (Andor Technology), with a frame size of 256 × 256 pixels and a corresponding pixel size of 160 nm. All imaging was performed using a Chroma Quad Band TIRF filter set (Chroma). Data collection was performed until exhaustion of the fluorophore population for all experiments, with molecule data shown for the noted frame ranges, corresponding to the length of the shortest run for each fusion. All data were collected at a frame rate of 6.7 Hz (150 ms/frame) with a camera EM gain multiplier value of 300, conversion gain value of 1, and without binning. Readout was performed using a 561 nm diode laser from an Agilent (Agilent Technologies) MLC400B monolithic laser combiner. Activation was performed using a 405 nm diode laser from the MLC400B, and applied as needed to ensure enough emitters were consistently being identified for the software drift correction algorithms to function properly (approximately 100 emitters identified per frame is considered ideal). The imaging buffer was a 10 mM cysteamine (MEA), 1% (w/v) polyvinyl alcohol solution in PBS.

Data analysis—Data collection and analysis was performed using Nikon's NIS-Elements 4.11 software. For analysis, only single emitters with an intensity of at least 300 gray levels above the local background were identified. Molecule data was further constrained to show statistics for molecules emitting between 50 and 5000 photons within the given frame range. Data was exported from the NIS Elements software into Microsoft Access (Microsoft Corporation) for database compilation and statistical analysis, followed by compilation of all statistical data into a single spreadsheet in Microsoft Excel for ease of reference.

Fixation and embedding for correlative light and electron microscopy—Cultured cells (3T3, CHO, HeLa) transfected with mEos4 variants were fixed after 24–48 hrs of expression with 4% PFA and 0.2% glutaraldehyde in 100 mM phosphate buffer, pH 7.2 (PB) on ice for 1 hr. After washing 3 × 3 min on ice, cells were scraped off and pelleted. The cell pellets were then processed for embedding in glycol methacrylate (GMA) in two approaches: conventional chemical fixation (CCF) with progressive lowering temperature (PLT) and high-pressure freezing / freeze substitution (HPS-FS).

For CCF, the cell pellets were resuspended in 1% agar and re-pelleted. After the agar solidified on ice, the pellet was cut into small pieces and post-fixed with OsO_4 and stained *en bloc* with 1% UA. The cell pellets were dehydrated with increasing concentrations of ethanol (EtOH) up to 95%, and then subjected to further dehydration and resin infiltration and embedding at −20°C. The GMA resin (low-acid GMA kit from SPI Supplies, West Chester, PA) was made up of GMA, n-butyl methacrylate (BMA), and benzoyl peroxide (BP), with no water. For a 20 ml stock solution (100%), 14 ml of GMA, 6 ml of BMA, 120 mg of BP were mixed in a glass vial. The water free-GMA is a modification of Watanabe *et al.* [11] method that better enables fluorescence detection and improves TEM morphology. After dehydration in 95% EtOH for 1 hr at −20 °C, the pellets were sequentially infiltrated

with 30% and 70% GMA (GMA stock solution diluted in 95% EtOH), each for 12 hrs. Further infiltration was carried out with 100% water-free GMA overnight followed by two more exchanges with 100% water-free GMA the following day. The pellets were embedded in pre-cooled 100% water-free GMA with N,N-dimethyl-p-toluidine (1.5 μl/ml GMA) in flat-bottom embedding capsules for two days. At the end of embedding, temperature was brought up from −20 °C to room temperature in 4 hrs.

For HPF-FS, the cell pellets were washed and resuspended in 20% BSA in PB. A small volume of the suspension (0.7 μl) was transferred to the 100 μm-deep well of a 0.1/0.2 mm specimen carrier (Type A, TechnoTrade International) and capped by the flat side of a Type B specimen carrier. The carrier assembly was high-pressure frozen with an HPF Compact 01 high-pressure-freezing machine (TechnoTrade International). The frozen carrier assembly was forced open in liquid nitrogen and the cells were freeze substituted in acetone with 0.1% uranyl acetate and OsO_4 at the specified concentration in a Leica EM AFS2 freeze substitution unit at −90 °C for 40 hours. After the temperature was brought up slowly to −20 °C, cells were rinsed with 95% EtOH six times over a period of 8 hrs, followed by sequential infiltration with 30% and 70% GMA in 95% EtOH for 12 hrs each. Further infiltration and embedding was performed as described for the CCF approach. The sample side of the specimen carrier faced up when embedded in the flat-bottom embedding capsule.

After temperature was returned to room temperature at the end of embedding, the sample blocks were removed from the embedding capsules. For samples embedded with the specimen carriers, the blocks were trimmed around the carriers, which were carefully removed with a pair of forceps after a brief cooling in liquid nitrogen. The exposed samples were further trimmed for ultra-thin sectioning.

Some samples were processed with EPON (Eponate 12 ™, Ted Pella) embedding as a control for structural preservation. Cells were processed as described in the CCF approach except that dehydration proceeded to pure EtOH at room temperature. After dehydration in pure EtOH for 3 × 10 minutes, samples were further dehydrated in propylene oxide 3 × 10 minutes. The samples were then infiltrated in mixtures of EPON and propylene oxide (1:1 then 2:1) for 1 hour each, pure EPON for two hours and then overnight. Final embedding was at 65 °C for 24 hours.

CLEM imaging—CLEM imaging was carried out using two complementary approaches: consecutive-section or same-section. For the consecutive-section approach, two consecutive sections were cut with a Leica UC6 ultra-microtome, with one (60 nm) on a Synaptek slot grid custom-coated with pioloform (1% in 1,2-dichloroethane) for EM imaging, and one (500 nm) picked up on a specially prepared coverslip for PALM imaging.

In this case PALM coverslips were prepared in the following way. First, 80 nm bare Au nanospheres (Microspheres-Nanospheres part# 790120-010) were deposited onto 25 mm #1.5 coverslips (Werner Instruments). Then a thin layer of Indium Tin Oxide (ITO) was sputtered over the sample using the Denton Explorer sputtering system (Denton Vacuum). The exact thickness of the ITO layer was not measured; instead we measured the electrical resistance between two point across the coverslip, which was ~2 kOhm. The optical loss of

the ITO layer was less than 5%. For the same-section approach, a 60 nm section was picked up on a coverslip spin-coated first with 80 nm Au nanospheres (same nanoparticles as in the consecutive section approach) and then with pioloform.

Typical PALM data acquisition consisted of 20,000-80,000 frames. We used iXon DU-897E EM-CCD cameras (Andor). Acquisition was performed in frame transfer mode; the laser excitation was constantly ON during acquisition. Activation light was generated from a CUBE 405-50 laser (Coherent), at 405 nm, 2–10 W/cm^2, with activation durations of 0.5–50 ms per imaging frame. Excitation light was generated from a CL561-150-O laser (CrystaLaser), at 561 nm, ~1000 W/cm^2. Exposure time was 50 ms. We used NF01-405/488/561/635 quad-notch filter (Semrock), LP02-568RU and FF01-593/40 filters (Semrock) as emission filters.

For the same-section approach, after PALM imaging, an area on the coverslip with the imaged section at the center was scored with a diamond knife without breaking the glass. The pioloform film was lifted by treatment with 1.2% hydrofluoric acid and floated on water in a glass Petri dish. An uncoated Synaptek slot grid was placed on the film, capturing the section in the center of the open slot. The grid was picked up by lifting the floating film with a piece of Parafilm. After drying, the grid was removed from the Parafilm and contrast stained with 3% UA and 1% Sato's triple lead. The grid was examined using an FEI Tecnai 20 TEM operated at 80kV. Cells imaged with PALM were located with positioning maps generated from the PALM imaging. Images were acquired with a Gatan Ultrascan 4k x 4k camera.

In the case of subsequent SEM imaging, the sample was then coated with 2 nm of Au/Pd alloy. The coating was performed using the Precision Etching and Coating System (Model 682 PECS; Gatan). This was followed by SEM imaging, which was performed using the Ultra SEM system (Carl Zeiss) with accelerating voltage of 1.5 KeV.

PALM-EM image registration was performed using Au nanoparticles. The same nanoparticles were observed under 561 nm illumination and in EM micrographs. This allowed for registration of two images using a POLYWARP 1 transformation defined by the equations [16]:

$$X' = Kx_{00} + Kx_{01} \cdot X + Kx_{10} \cdot Y + Kx_{11} \cdot X \cdot Y$$
$$Y' = Ky_{00} + Ky_{01} \cdot X + Ky_{10} \cdot Y + Ky_{11} \cdot X \cdot Y$$

Typical average PALM-EM registration error was ~5 nm.

Quantification of localization precision in CLEM imaging—PALM data sets were analyzed from Fig. 3c (mitochondrial mEos4a) and Fig. 3b (lamin A-mEos4b); both were secondary-fixed with the 0.5% OsO_4 used for HPF-FS. A lamin B1-mEos2 PALM data set was taken from Fig. 3 from reference [13]. Equation (6) from reference [45] was used to estimate the localization precision of each fluorescent event in each data set. The sets of all individual localization precision estimates for each of the three experiments were then assembled into normalized distributions (of fluorescent molecule counts), which were

analyzed in Microsoft Excel to yield median single-molecule localization precision values for each experiment. Results are shown in Supplementary Fig. 8.

Testing mEos fluorescence survival in EPON epoxy resin—Constructs driving mitochondrial mEos2, mEos4a or mEos4b expression (same as those used in Fig. 3) were transfected into 3T3 cells and allowed to express for 24 hours. After mEos expression, cells were primary-fixed with 4% PFA / 0.2% glutaraldehyde and secondary-fixed with 1% OsO_4, dehydrated in 100% ethanol and finally resin infiltrated with EPON (Eponate 12 ^{TM}, Ted Pella). 100 nm sections were then cut on an ultramicrotome and imaged on an epifluorescence microscope. Images were acquired on a Nikon Eclipse Ti Inverted microscope with a CFI Plan Apo Lambda 60x oil-immersion objective, numerical aperture 1.4. Light source was a SPECTRA X light engine (Lumencor), with excitation centered around 470 nm for the green channel and 555 nm for the red channel. Emission light was collected with 515/30 nm and 595/40 nm bandpass filters, respectively. Through the microscope objective, all six images looked completely black. To show that cells were present and in focus in the fields of view, 16-bit images were taken on a Zyla 4.2 sCMOS camera (Andor) and adjusted in ImageJ to artificially enhance contrast. Histogram adjustment to show very dim fluorescent pixels clearly reveals section edges (visible at top of each field of view), as well as 3T3 cells (the dark excluded regions). Results are shown in Supplementary Fig. 9.

Testing red, photoconverted mEos survival in 1% OsO_4—HeLa cells transfected with plasmids encoding cytoplasmic mEos variants were allowed to express for 24 hours and then photoconverted on the stage of a Nikon Eclipse Ti Inverted microscope with a CFI Plan Apo Lambda 10x objective, numerical objective 0.45. Photoconversion was performed with light from a SPECTRA X light engine (Lumencor) source filtered through the microscope's DAPI filter set, with 10-second exposure time. Following photoconversion, images in the red channel were acquired through the same objective, with excitation centered at 555 nm and emission light collected through a 595/40 nm bandpass filter set. Cells were then primary-fixed by addition of 4% PFA / 0.2% glutaraldehyde and a second set of images were acquired. Finally, cells were secondary-fixed by addition of 1% OsO_4 in a fume hood, washed three more times with water, after which a cover slip was added and the slide taken back to the microscope. A third set of images was acquired, in which fields of view were effectively black. All three mEos variants were acquired with identical camera settings. Results are shown in Supplementary Fig. 10.

REPRODUCIBILITY STATEMENT

Sample sizes were chosen to be sufficient to show the magnitude of effects of the different treatments. Effects were large and qualitative and did not require statistical analysis of significance. No data were excluded.

Supplementary Material

Refer to Web version on PubMed Central for supplementary material.

Acknowledgments

We would like to thank D. Murphy and R. Fetter for helpful discussions. E. Betzig generously allowed use of his PALM scope early in the project. S. Winfrey, H. White and A. Tkachuk assisted with cell culture. B. Kopek gave advice and technical support on PALM and CLEM. P. Rivlin gave advice on EM. P. Hulamm, L. Shao and T.-L. Chew provided technical support for imaging. T. Gallagher, M. Ramirez, P. Nguyen and K. McGowan aided in molecular biology. J. Marvin, J. Akerboom, M. Verdecia and E. Schreiter provided advice on biochemical characterization techniques. S. McKinney was helpful in the design of the anisotropy assay. Several members of the Davidson laboratory (FSU) assisted with characterization of the protein fusions: P. Cranfill, B. Sell, L. Case, J. Shirley, S. Gilbert, K. Hendrickson, R. Labaddan and R. Clarke. M.G.P.S. would like to thank M. Reddy for guidance and mentoring in biochemistry and molecular biology.

References

1. Shaner NC, Patterson GH, Davidson MW. J Cell Sci. 2007; 120:4247–4260. [PubMed: 18057027]
2. Lippincott-Schwartz J, Patterson GH. Trends Cell Biol. 2009; 19:555–565. [PubMed: 19836954]
3. Huang B. Curr Opin Chem Biol. 2010; 14:10–14. [PubMed: 19897404]
4. Betzig E, et al. Science. 2006; 313:1642–1645. [PubMed: 16902090]
5. Hess ST, Girirajan TP, Mason MD. Biophys J. 2006; 91:4258–4272. [PubMed: 16980368]
6. Wiedenmann J, et al. Proc Natl Acad Sci USA. 2004; 101:15905–15910. [PubMed: 15505211]
7. Nienhaus GU, et al. Photochem Photobiol. 2006; 82:351–358. [PubMed: 16613485]
8. McKinney SA, Murphy CS, Hazelwood KL, Davidson MW, Looger LL. Nat Methods. 2009; 6:131–133. [PubMed: 19169260]
9. Zhang M, et al. Nat Methods. 2012; 9:727–729. [PubMed: 22581370]
10. Shroff H, Galbraith CG, Galbraith JA, Betzig E. Nat Methods. 2008; 5:417–423. [PubMed: 18408726]
11. Watanabe S, et al. Nat Methods. 2011; 8:80–84. [PubMed: 21102453]
12. Tokuyasu KT. J Cell Biol. 1973; 57:551–565. [PubMed: 4121290]
13. Kopek BG, Shtengel G, Xu CS, Clayton DA, Hess HF. Proc Natl Acad Sci USA. 2012; 109:6136–6141. [PubMed: 22474357]
14. Chang YW, et al. Nat Methods. 2014; 11:737–739. [PubMed: 24813625]
15. Collins JS, Goldsmith TH. J Histochem Cytochem. 1981; 29:411–414. [PubMed: 6787116]
16. Kopek BG, Shtengel G, Grimm JB, Clayton DA, Hess HF. PloS ONE. 2013; 8:e77209. [PubMed: 24204771]
17. Li J, Wang Y, Chiu SL, Cline HT. Front Neural Circuits. 2010; 4:6. [PubMed: 20204144]
18. Martell JD, et al. Nat Biotech. 2012; 30:1143–1148.
19. Shu X, et al. PLoS Biology. 2011; 9:e1001041. [PubMed: 21483721]
20. Rust MJ, Bates M, Zhuang X. Nat Methods. 2006; 3:793–795. [PubMed: 16896339]
21. Micheva KD, Smith SJ. Neuron. 2007; 55:25–36. [PubMed: 17610815]
22. Berning S, Willig KI, Steffens H, Dibaj P, Hell SW. Science. 2012; 335:551. [PubMed: 22301313]
23. Ando R, Mizuno H, Miyawaki A. Science. 2004; 306:1370–1373. [PubMed: 15550670]
24. Adam V, et al. Proc Natl Acad Sci USA. 2008; 105:18343–18348. [PubMed: 19017808]
25. Robertson CE. Methods Cell Biol. 2007; 79:169–191. [PubMed: 17327157]
26. Kozak M. J Mol Biol. 1987; 196:947–950. [PubMed: 3681984]
27. Creighton, TE. Proteins: Structures and Molecular Properties. 2. W.H. Freeman; New York: 1993.
28. Nienhaus K, Nienhaus GU, Wiedenmann J, Nar H. Proc Natl Acad Sci USA. 2005; 102:9156–9159. [PubMed: 15964985]
29. Habuchi S, Tsutsui H, Kochaniak AB, Miyawaki A, van Oijen AM. PloS ONE. 2008; 3:e3944. [PubMed: 19079591]
30. Kunkel TA. Proc Natl Acad Sci USA. 1985; 82:488–492. [PubMed: 3881765]
31. Studier FW. Protein Expr Purif. 2005; 41:207–234. [PubMed: 15915565]
32. Schuck P. Biophys J. 2000; 78:1606–1619. [PubMed: 10692345]

33. Costantini LM, Fossati M, Francolini M, Snapp EL. Traffic. 2012; 13:643–649. [PubMed: 22289035]
34. Brown TA, Fetter RD, Tkachuk AN, Clayton DA. Methods. 2010; 51:458–463. [PubMed: 20060907]
35. Hayat, MA. Principles and Techniques of Electron Microscopy: Biological Applications. 4. Cambridge University Press; Cambridge: 2000.
36. Clancy B, Cauller LJ. J Neurosci Meth. 1998; 83:97–102.
37. Beckstead JH. J Histochem Cytochem. 1994; 42:1127–1134. [PubMed: 8027531]
38. Lomant AJ, Fairbanks G. J Mol Biol. 1976; 104:243–261. [PubMed: 957432]
39. Mattson G, et al. Mol Biol Rep. 1993; 17:167–183. [PubMed: 8326953]
40. Tokumasu F, Dvorak J. J Microsc. 2003; 211:256–261. [PubMed: 12950474]
41. Hand AR, Hassell JR. J Histochem Cytochem. 1976; 24:1000–1011. [PubMed: 61239]
42. Lakowicz, JR. Principles of Fluorescence Spectroscopy. 3. Springer; New York: 2011.
43. Beisker W, Dolbeare F, Gray JW. Cytometry. 1987; 8:235–239. [PubMed: 3582069]
44. Phillips SR, Wilson LJ, Borkman RF. Curr Eye Res. 1986; 5:611–619. [PubMed: 3757547]
45. Mortensen KI, Churchman LS, Spudich JA, Flyvbjerg H. Nat Methods. 2010; 7:377–381. [PubMed: 20364147]

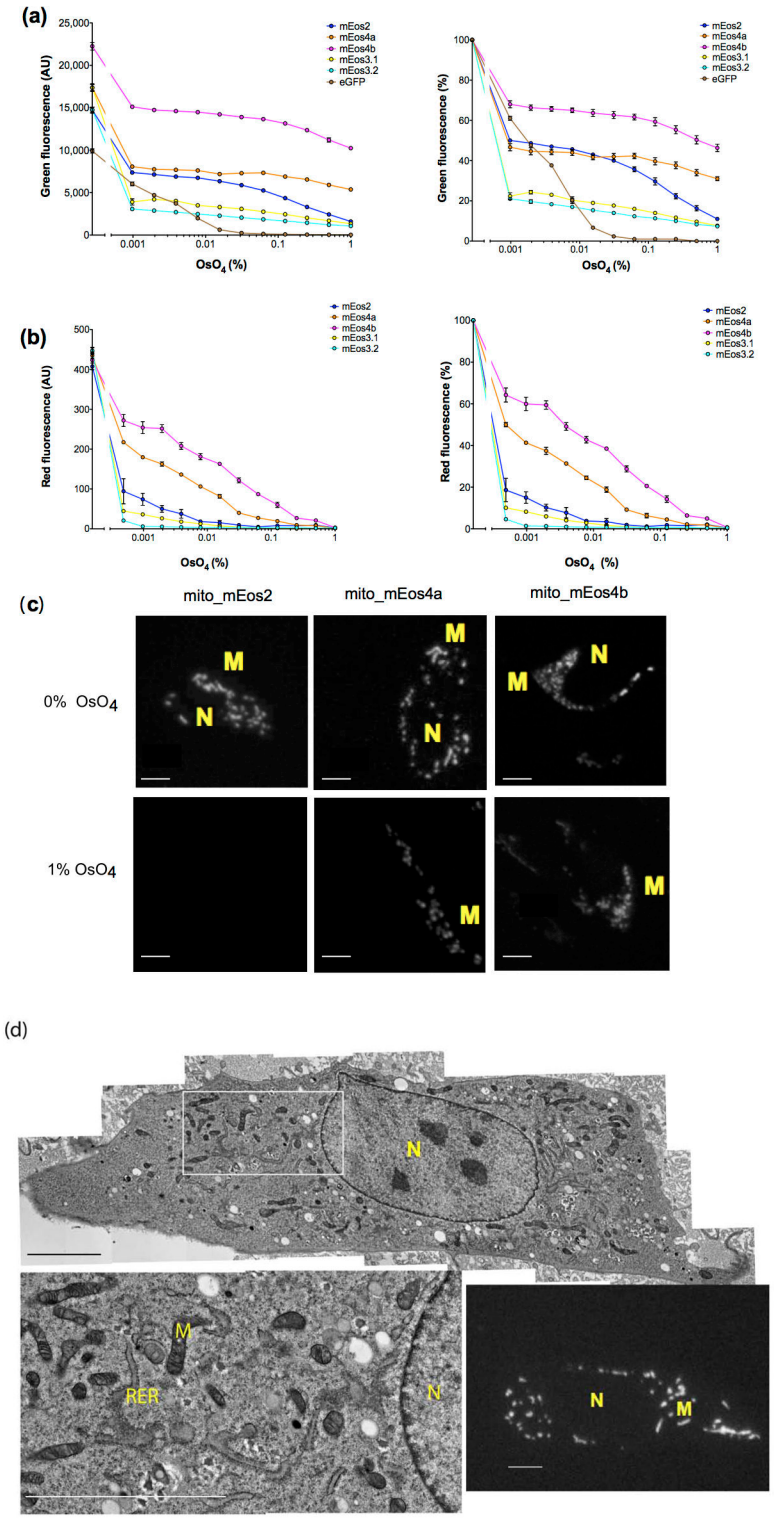

Figure 1.

Osmium resistance of the mEos4 probes. a) Green mEos (and eGFP; 1 μM) fluorescence preservation in OsO_4 (incubation for 10 minutes before measurement). Excitation 480 nm, emission 515 nm, bandwidths 5 nm. Left, raw fluorescence values, all at same fluorimeter

settings. Right, normalized data. b) Photoconversion of Eos (1 μM) from green to red in the presence of OsO_4 (incubation/photoconversion for 30 minutes before measurement). Excitation 550 nm, emission 580 nm, bandwidths 5 nm. Left, raw fluorescence values, all at same fluorimeter settings. Right, normalized data. See **Methods** for details of normalization. Mean and s.e.m. shown: $n = 3$. c) Fluorescence preservation of mitochondrially expressed mEos variants in fixed 3T3 cells, post-fixed with 1% OsO_4 and embedded in GMA. 60 nm GMA sections, 100 ms exposure time. Scale bars, 5 μm. See **Methods** for details of background subtraction. d) TEM images of 3T3 cells expressing mitochondrial mEos4a. Cells were post-fixed in 1% OsO_4 and embedded in GMA. EM images are of 40 nm-thick sections. Top: montage reconstruction of whole cell from tiled images. Bottom left: zoomed TEM image, showing mitochondria (M- note cristae), rough endoplasmic reticulum (RER- note ribosomes), and nuclear envelope (N- note bilayer). Bottom right: fluorescence image of a 60 nm-thick section from same cell, cut after the 40 nm-thick section used for TEM. Scale bars, 5 μm.

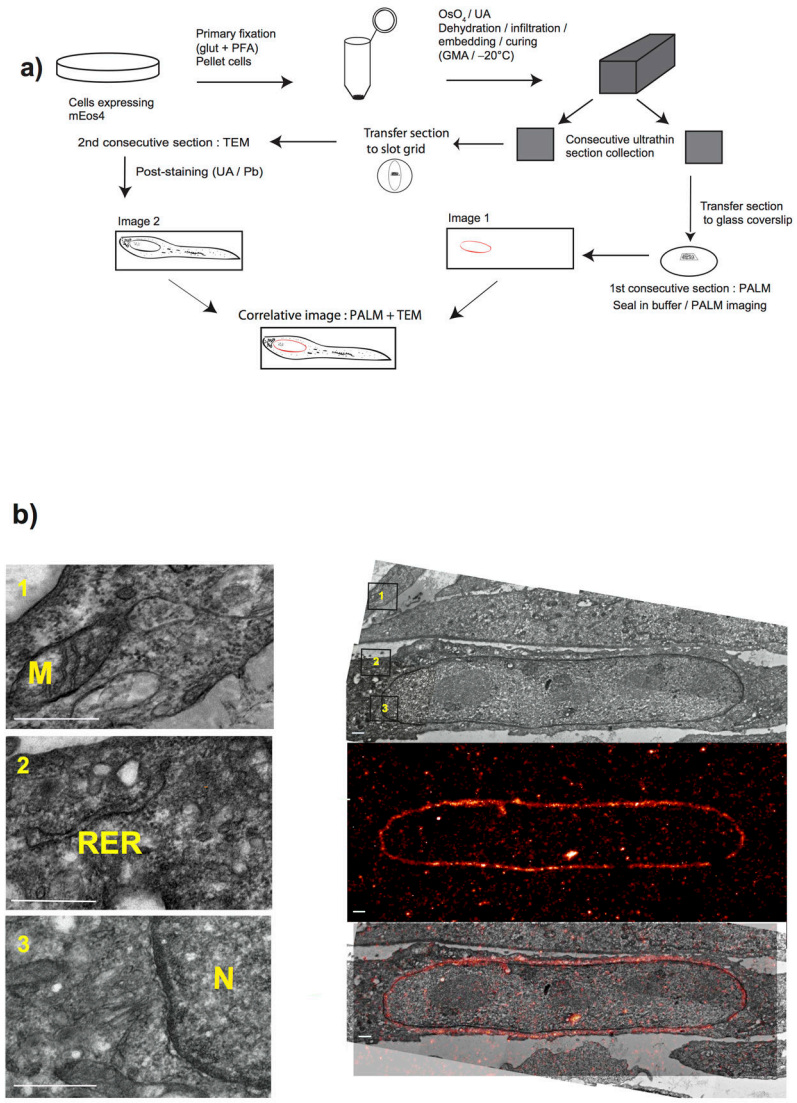

Figure 2.

Correlative PALM and TEM imaging using the consecutive-section approach. a) Schematic of consecutive-section approach using conventional chemical fixation. glut = glutaraldehyde, UA = uranyl acetate, Pb = Sato's triple lead. b) Top right: A montage of TEM images of a 60 nm GMA section of a 3T3 cell expressing mEos4b-lamin A. Cells were postfixed with 1% OsO_4 and embedded in GMA. Middle right: PALM image of a 500 nm section cut consecutively to the 60 nm section, showing localization of mEos4b-lamin A. Bottom right: manual overlay of PALM and TEM images. Left: zoomed images of boxed areas, showing mitochondrial cristae, ribosomes and nuclear bilayer. Scale bars, 500 nm.

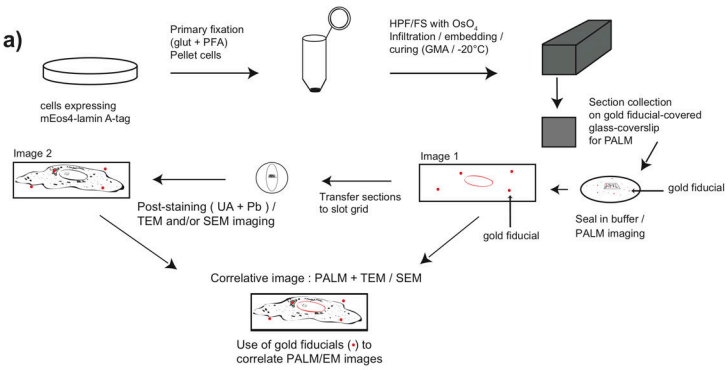

b)

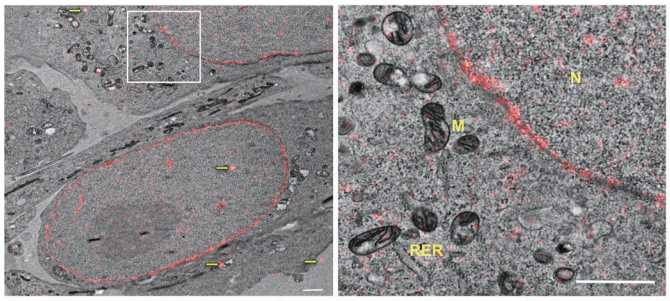

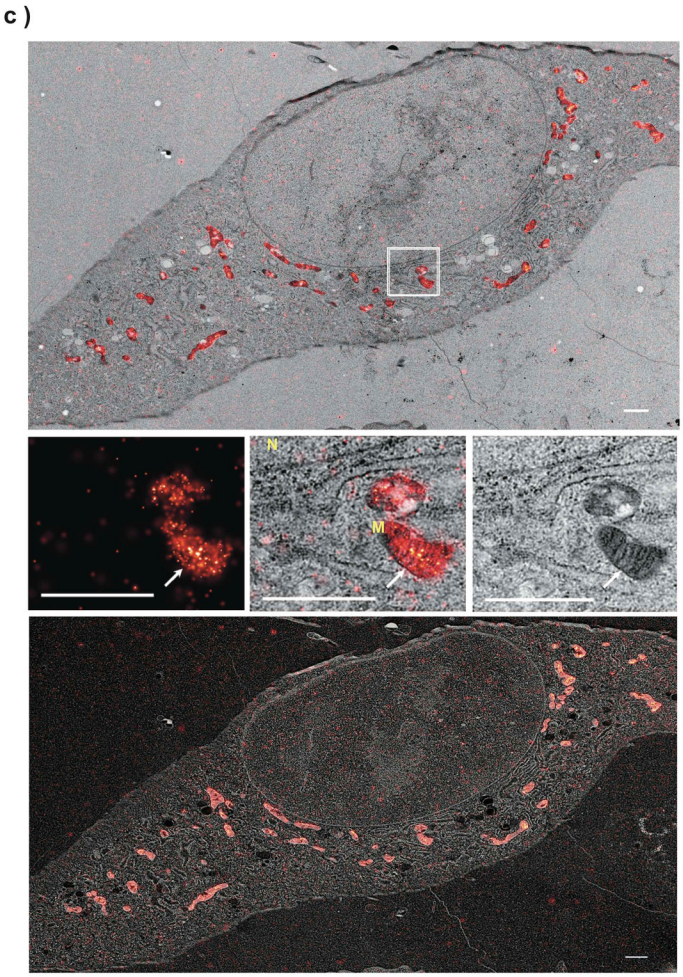

Figure 3.

Correlative PALM and TEM/SEM imaging using the same-section approach. a) Schematic of same-section approach using HPF-FS. glut = glutaraldehyde, UA = uranyl acetate, Pb = Sato's triple lead. b) Left: Overlaid PALM (red) and TEM images taken on 60 nm GMA section of 3T3 cells expressing mEos4b-Lamin A. 0.5% OsO_4. Right: Zoomed image of the marked area. Scale bars, 1 μm. Yellow arrows indicate fluorescent, electron-dense gold nanoparticles used for fiducial registration. c) CLEM images of 60 nm GMA section of 3T3 cells expressing mitochondrially targeted mEos4a. 0.5% OsO_4. Top: whole cell. Middle: PALM, merge and TEM images of boxed area. Arrow indicates a mitochondrial cristae fold. Bottom: Overlaid PALM and SEM images of the same section. Scale bars, 1 μm. N = nucleus, M = mitochondrion, RER = rough endoplasmic reticulum.